Supporting information for

Dual-productive photoredox cascade catalyst for solar hydrogen production and methylarene oxidation

*Atsushi Kobayashi**

Department of Chemistry, Faculty of Science, Hokkaido University, North-10 West-8, Kita-ku, Sapporo 060-0810, Japan, akoba@sci.hokudai.ac.jp

Contents

References

Experimental Section

Materials and Syntheses

Caution! *Although we did not come across any difficulties, most of the chemicals used in this study are potentially harmful and should be used in small quantities and handled with care in a fume hood.* All commercially available starting materials were used as received without further purification. The TiO_2 nanoparticles (CSB, ~7 nm in diameter) were purchased from Sakai Chemical Industry Co. Ltd. Pt-TiO_2 (1.4 wt%) was prepared using a previously reported photodeposition method.[R1] Ru(II) molecular photosensitizers (**RuCP^6** and **RuP^6**) were synthesized using previously reported methods. [R2]

Preparations of single- and dual-dye sensitized photocatalysts (SDSP and DDSP)

Single- and dual-dye sensitized Pt-TiO_2 photocatalysts, Zr^{4+}-**RuP^6**@Pt-TiO_2, and Hf^{4+}-**RuCP^6**-Zr^{4+}-**RuP^6**@Pt-TiO_2 (SDSP, and DDSP) were synthesized by our previous procedure[R3] for Ru(II)-dye-immobilized Pt-TiO_2 nanoparticles with several modification as follows. The immobilized amount of each Ru(II) PS was estimated by the UV-vis absorption spectrum of each supernatant isolated by the ultracentrifugation of Ru(II) PS immobilization reaction (**Figure S1** and **Table S1**).

I. Immobilization of the first **RuP^6** dye. 30 mg of Pt-TiO_2 nanoparticles were added and dispersed in ca. 2.5 mM **RuP^6** solution (6 mL). A 50 μL of 70%$HClO_4$ aq. solution was added to the dispersion solution and stirred overnight at 293 K in dark condition. The Ru(II)-dye-immobilized Pt-TiO_2 nanoparticles were isolated by ultracentrifugation (50,000 rpm, 15 min) and then twice washed with 0.1 mM $HClO_4$ aq. The **RuP^6**@Pt-TiO_2 were obtained by drying in air at 313 K for one night.

II. Immobilization of Zr^{4+} cations to the phosphonates of Ru(II) dyes. The well dried **RuP^6**@Pt-TiO_2 nanoparticles were dispersed in 6 mL of MeOH solution of 20 mM $ZrCl_2O{\cdot}8H_2O$ and stirred for 1 h at 293 K in dark condition. The dispersed nanoparticles were collected by ultracentrifugation (50,000 rpm, 15 min) washed twice with MeOH, and then dried under air for one night at 313 K to afford the orange-colored SDSP, Zr^{4+}-**RuP^6**@Pt-TiO_2.

III. Immobilizations of the second **RuCP^6** dye and surface Hf^{4+} cations. The second immobilization of Ru(II) dye was conducted in the almost the same procedure to that used for the first layer immobilization as mentioned above by using Zr^{4+}-**RuP^6**@Pt-TiO_2 nanoparticles instead of Pt-TiO_2. The SDSP (Zr^{4+}-**RuP^6**@Pt-TiO_2) nanoparticles were dispersed in ca. 2.5 mM **RuCP^6** solution (6 mL) and then acidified by addition of a 50 μL of 70%$HClO_4$ aq. solution. After stirring overnight at 293 K in dark condition, the dispersed nanoparticles were isolated by ultracentrifugation (50,000 rpm, 15 min) and then twice washed with 0.1 mM $HClO_4$ aq. The **RuCP^6**-Zr^{4+}-**RuP^6**@Pt-TiO_2 nanoparticles were obtained by drying in air for one night at 313 K. Further treatment of **RuCP^6**-Zr^{4+}-**RuP^6**@Pt-TiO_2 nanoparticles with $HfCl_2O{\cdot}8H_2O$ MeOH solution as mentioned above (see II. Immobilization of Zr^{4+} cations to the phosphonates of Ru(II) dyes) was conducted to form the Hf^{4+}-cation modified Ru(II)-dye-double-layered nanoparticle Hf^{4+}-**RuCP^6**-Zr^{4+}-**RuP^6**@Pt-TiO_2 (DDSP).

Measurements

UV−vis absorption spectra were recorded on a JASCO V-750 spectrophotometer. Emission spectra were recorded on a JASCO FP-8550 spectrofluorometer at 298 K and each sample solution was deoxygenated by N_2 bubbling for 30 min at 293 K. Energy-dispersive XRF spectra were recorded using a Bruker S2 PUMA analyzer. ^{1}H- and ^{13}C-NMR spectra at room temperature were recorded on an ECZ-400S NMR spectrometer. Powder X-ray diffraction studies were conducted using a Bruker D8 Advance diffractometer equipped with a graphite monochromator employing Cu Kα radiation and a one-dimensional LynxEye detector.

Photocatalytic water reduction reaction

Under dark conditions, a CH_3CN solution containing NHPI, pyridine (50 mM), 0.1 M substrate (ethylbenzene, cyclohexene, toluene or toluene-d_8) and DDSP nanoparticles (100 μM of the Ru(II) dye) was placed into a homemade Schlenk flask-equipped quartz cell (volume: 145 mL) with a small magnetic stirring bar. Each sample flask was doubly sealed with rubber septa. This mixed solution was deoxygenated by Ar bubbling for 1 h. The flask was then irradiated from the side and bottom with two blue LED lamps (λ = 467 ± 30 nm; 550 mW; HepatoChem Ltd., HCK1012-01-32). The temperature was controlled at 293 K using an air circulating system (HepatoChem Ltd., HCK1006-01-023). The gas samples (0.6 mL) for each analysis were collected from the headspace using a gastight syringe (Valco Instruments Co. Inc.). The amount of evolved H_2 was determined using a gas chromatograph (Agilent 490 Micro Gas Chromatograph). The turnover number and turnover frequency per Ru dye (PS TON and PS TOF) were estimated from the amount of evolved H_2; two photoredox cycles of the Ru(II) PS are required to produce one H_2 molecule. Each photocatalytic H_2 evolution reaction was conducted under the same conditions three times, and the average value with standard deviation is reported. The detection limit of this gas chromatography analysis for H_2 gas was 0.05 μmol. The AQY was calculated using the following equation:

$$AQY = N_e/N_p = 2N_{H2}/ N_p,$$

Here, N_e represents the number of reacted electrons, N_{H2} is the number of evolved H_2 molecules, and N_p is the number of incident photons.

Calculation of the amount of Ru(II) complex immobilized on the Pt-TiO_2 nanoparticles

To estimate the amount of immobilized Ru(II) complexes on Pt-TiO_2 nanoparticle, UV-vis absorption spectra of each supernatant solution used for the immobilization reaction was measured (**Figure S1**). The Ru(II) complex concentration used for the UV-Vis absorption spectral measurement (C_A) is estimated by Equation (1) based on the Lambert-Beer law.

$$A = C_A \cdot l \cdot \varepsilon \quad (Eq.\ 1)$$

A = absorbance, C_A = concentration of the Ru(II) complex,

l = cell path length (1 cm), ε = molar absorption coefficient

The absorbance at the ^{1}MLCT absorption band of each complex (**RuP**^{6}: 464 nm, **RuCP**^{6}: 465 nm) and their corresponding molar absorption coefficients (**RuP**^{6}: 16,350; **RuCP**^{6}: 14,249) enable us to estimate the concentration of the Ru(II) complex that was not immobilized in the reaction. Since a 50-fold diluted aqueous solution was used in each measurement, the concentration of the original supernatant solution (C_B) is calculated by $C_B = C_A \times 50$. The total volume of the supernatant solution is 6.05 mL (see "Preparation of dual-dye-sensitized photocatalyst" section). Thus, the amount of Ru(II) complexes in the supernatant solution (M_S) is estimated by Equation (2).

$$M_s = C_B \times \frac{6.05}{1000}\ (\text{mol}) \quad (Eq.\ 2)$$

Finally, the molar amount of the Ru(II) complex immobilized on the TiO_2 surface (M_i) can be estimated by Equation (3).

$$M_i = M_o - M_s\ (\text{mol}) \quad (Eq.\ 3)$$

where M_o denotes the molar amount of the Ru(II) complex in the stock solution of Ru(II) complex used for the immobilization reaction. The results are summarized in **Table S1**.

Calculation of the surface coverage of Ru(II) complexes per unit area of TiO_2

Assuming that the TiO_2 nanoparticles are spherical, we simply calculated the surface area on the TiO_2 nanoparticle (S_m) using Equation (4). In these calculations, the effect of the loaded Pt co-catalyst was omitted.

$$S_m = 4 \cdot \pi \cdot \left(\frac{a}{2} \times 10^{-7}\right)^2 \ (\mathrm{cm^2\ per\ one\ particle}) \ \ (Eq.\ 4)$$

a = Averaged particle diameter of TiO_2 nanoparticle (7 nm)

Since the calculated surface area (S_m) based on Equation (4) corresponds to only one TiO_2 nanoparticle, it is necessary to determine the number of TiO_2 nanoparticles (P_t) contained in 30 mg to estimate the total surface area of TiO_2 (S_t) used in the immobilization reaction of the Ru(II) complexes. The total volume of 30 mg of TiO_2 nanoparticles (V_t) can be calculated using Equation (5) based on the density of TiO_2 (anatase TiO_2 = 3.90 g/cm^3).

$$V_t = \frac{30 \times 10^{-3}\ (\mathrm{g})}{3.90\ (\mathrm{g/cm^3})}\ (\mathrm{cm^3}) \ \ (Eq.\ 5)$$

The number of TiO_2 nanoparticles (P_t) in 30 mg is also estimated using Equations (6) and (7) based on the volume of one TiO_2 nanoparticle (V_m) and the total volume (V_t).

$$V_m = \frac{4}{3} \cdot \pi \cdot \left(\frac{a}{2} \times 10^{-7}\right)^3 \ (\mathrm{cm^3\ per\ one\ particle}) \ \ (Eq.\ 6)$$

$$P_t = \frac{V_t}{V_m} \ \ (Eq.\ 7)$$

Then, the total surface area of 30 mg of TiO_2 (S_t) can be estimated by Equation (8).

$$S_t = S_m \times P_t\ (\mathrm{cm^2}) \ \ (Eq.\ 8)$$

The amount of immobilized Ru(II) complexes per unit area of TiO_2 (Surface coverage: N) is estimated by Equation (9) based on the amount of immobilized Ru(II) complex (M_i) and the total surface area of 30 mg of TiO_2 (S_t). The estimated N and M_i values are summarized in **Table S1**.

$$N = \frac{M_i}{S_t}\ (\mathrm{mol/cm^2}) \ \ (Eq.\ 9)$$

Table S1. Absorbance of each stock and supernatant solutions and the M_o, M_s, and M_i values of DDSP = Hf^{4+}-**RuCP^6**-Zr^{4+}-**RuP^6**@Pt-TiO_2.

Photocatalyst	Immobilized Ru(II) PS	A_{stock}	M_o (μmol)	A_{super}	M_s (μmol)	M_i (μmol)	Surface coverage N (nmol / cm^2)	Footprint (nm^2)
DDSP	1st (inner) layer **RuP^6**	0.9396	17.63	0.2300	4.316	13.31	0.2018	0.8227
	2nd (outer) layer **RuCP^6**	0.8313	17.89	0.5471	11.78	6.110	0.09277	1.791

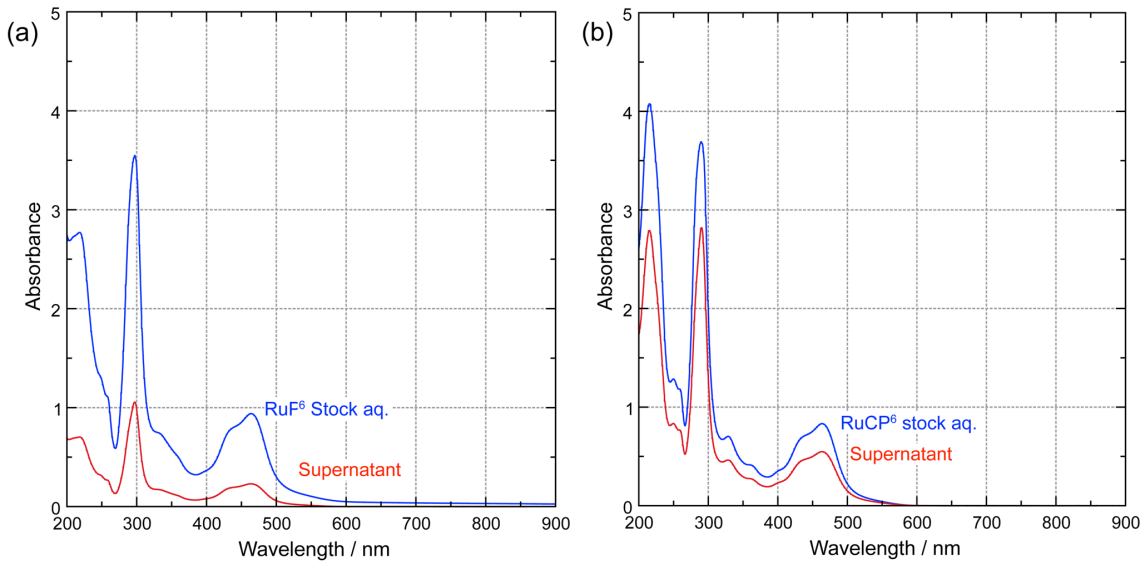

Figure S1. UV-vis absorption spectra of the stock and supernatant (blue and red lines) solutions obtained during the preparations of (a) Zr^{4+}-**RuP^6**@Pt-TiO_2 (SDSP) and (b) Hf^{4+}-**RuCP^6**-Zr^{4+}-**RuP^6**@Pt-TiO_2 (DDSP) at 298 K.

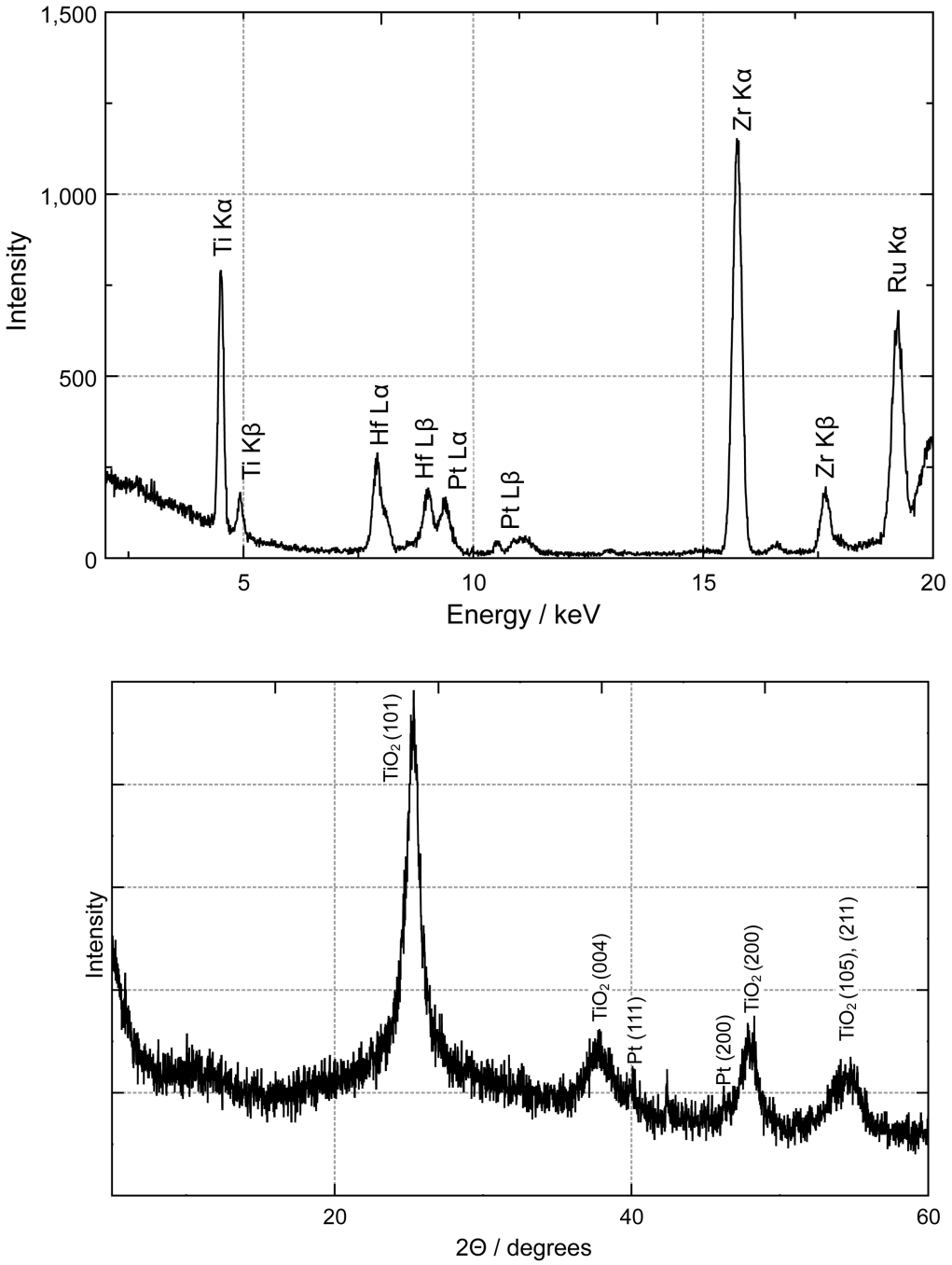

Figure S2. (top) Solid-state XRF spectrum and (bottom) powder XRD pattern of Hf^{4+}-**RuCP^{6}**-Zr^{4+}-**RuP^{6}**@Pt-TiO_2 (DDSP) at 298 K in air.

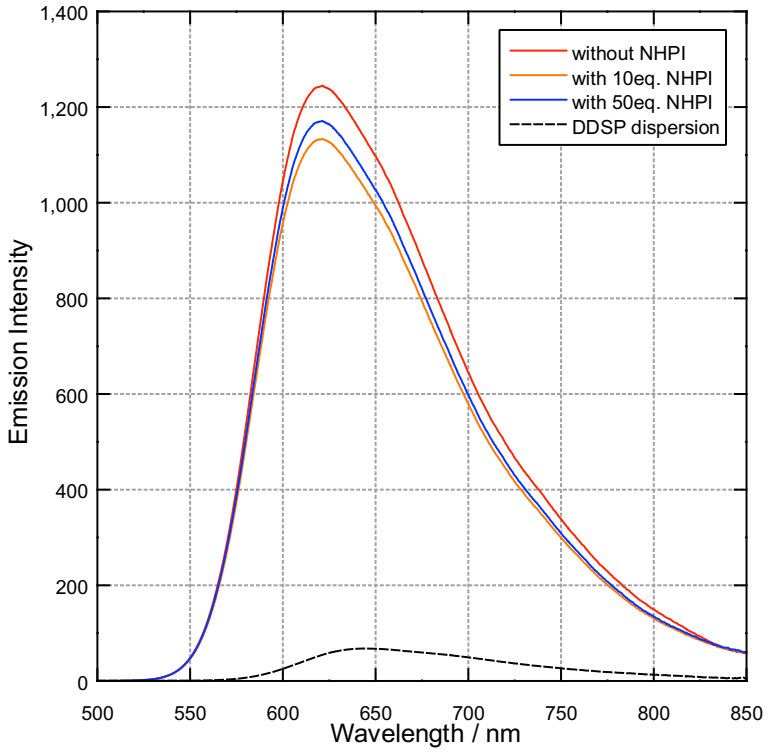

Figure S3. Emission spectra of CH_3CN solution of 100 μM $[Ru(bpy)_3]Cl_2$ in the presence of 0 to 50 mM NHPI at 293 K. Black dashed line shows the spectrum of DDSP dispersed in CH_3CN ([Ru] = 100 μM) obtained in the same experimental condition. (λ_{ex} = 465 nm)

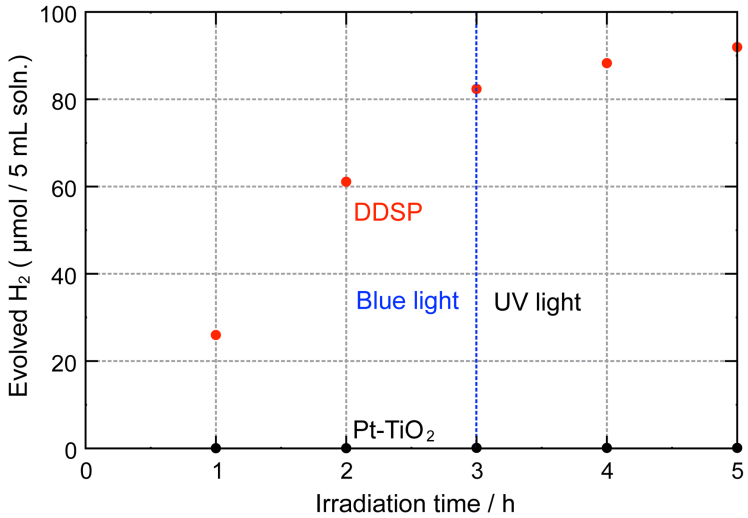

Figure S4. Photocatalytic H_2 evolution by DDSP (red; Ru(II) dye concentration was 100 μM) or Pt-TiO_2 (black; the amount was 1.04 mg that is almost equal to the amount of Pt-TiO_2 in DDSP) in the presence of 30 mM NHPI, 50 mM pyridine, and 0.1 M ethylbenzene (EB) in CH_3CN under blue or UV light irradiation (λ = 470 ± 30 nm, 110 mW for 0-3 h, and 365 ± 20 nm, 95 mW for 3-5 h).

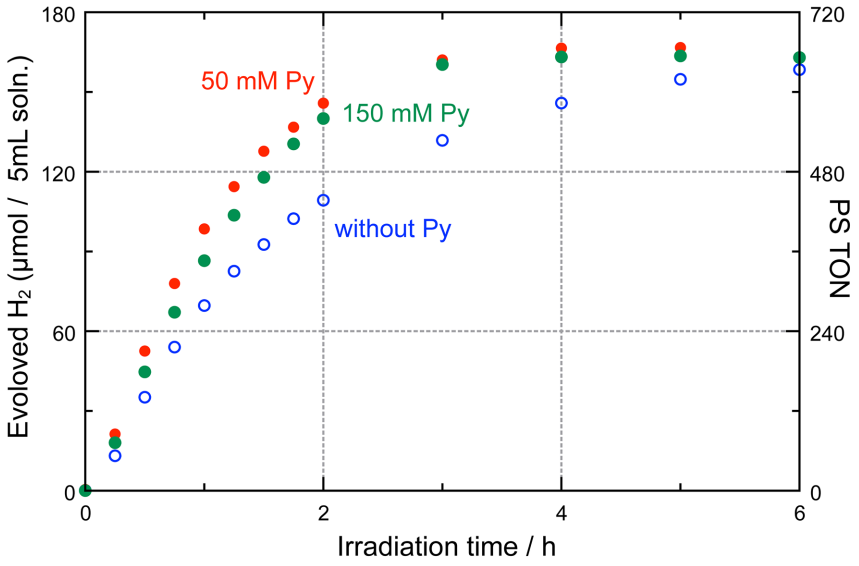

Figure S5. Photocatalytic H_2 evolution by DDSP in the presence of 30 mM NHPI and 0.1 M ethylbenzene (EB) CH_3CN solution under blue-light irradiation (λ = 467 ± 30 nm; 550 mW) in the (blue open circle) absence or presence of (red) 50, (green) 150 mM pyridine. The Ru(II) dye concentration was 100 µM for all reactions.

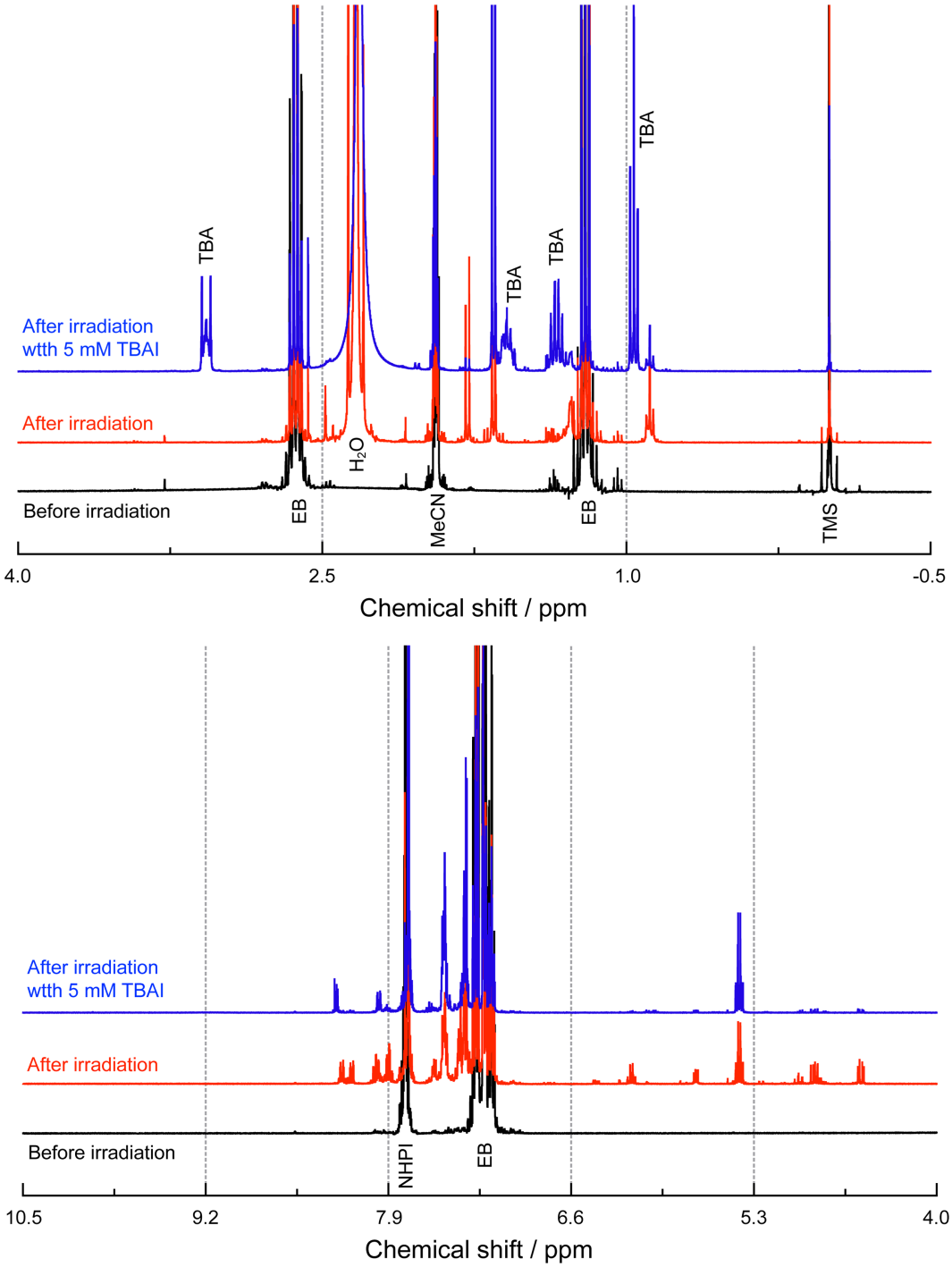

Figure S6. Comparison of ^{1}H NMR spectra (top and bottom: aliphatic and aromatic regions) of CD_3CN solution containing 30 mM NHPI, 50 mM pyridine-d^5, and 0.1 M ethylbenzene (black) before and (red) after 5 h light irradiation with DDSP ([Ru] = 100 μM). Blue lines show the spectra of the solution obtained by the 18 h photocatalytic H_2 evolution reaction in the presence of 5 mM tetrabutylammonium iodide (TBAI).

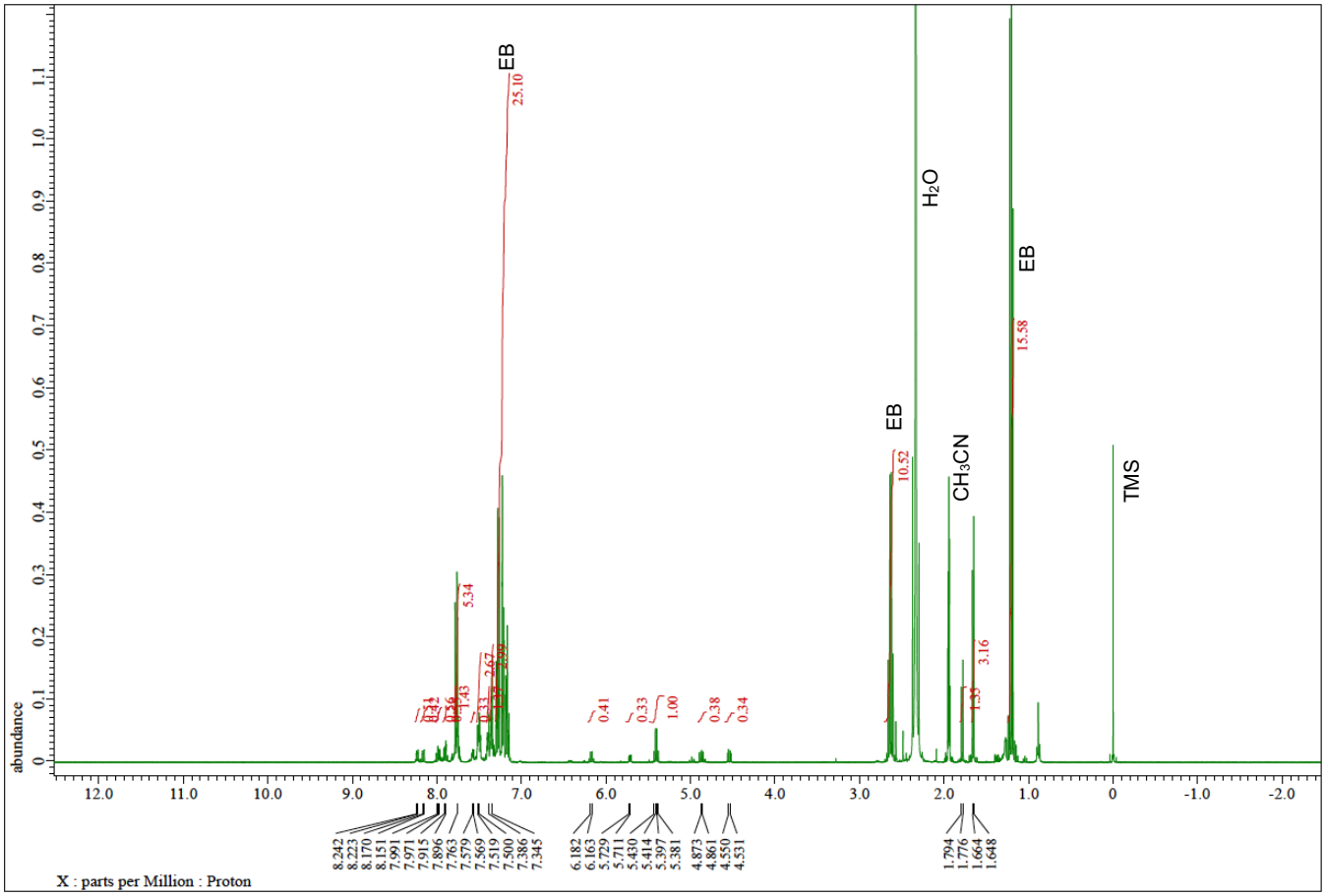

Figure S7. ^{1}H NMR spectra of the reaction supernatant obtained by 5 h photocatalytic H_2 production in the presence of DDSP ([Ru] = 100 μM), 30 mM NHPI, 50 mM pyridine-d^5, and 0.1 M ethylbenzene in CD_3CN.

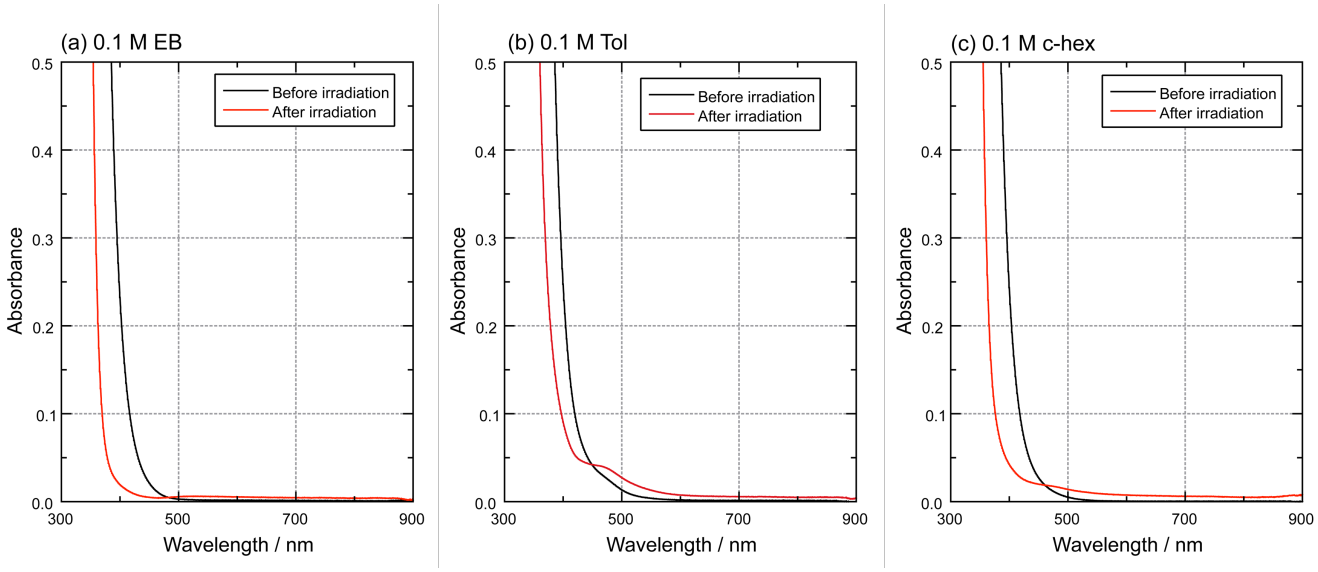

Figure S8. UV-vis absorption spectra of the reaction supernatant (black) before and (red) after photocatalytic H_2 evolution reaction by DDSP for 5 h in the presence of 30 mM NHPI, 50 mM pyridine and 0.1 M (a) ethylbenzene (EB), (b) toluene (Tol), or (c) cyclohexene (*c*-hex), CH_3CN solution.

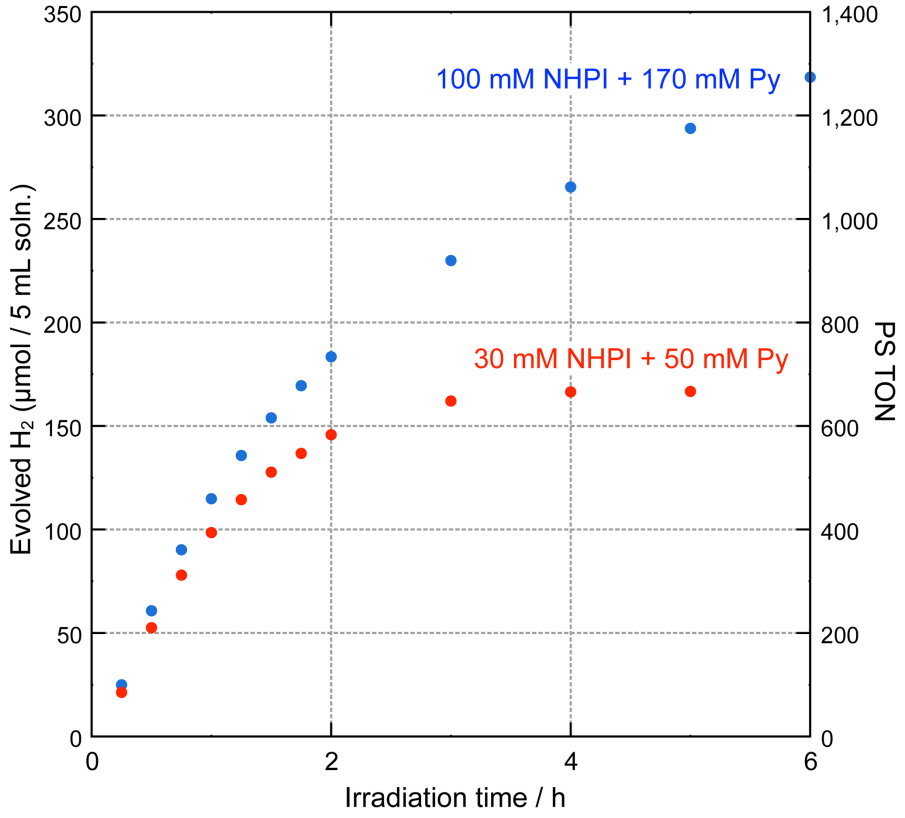

Figure S9. Photocatalytic H_2 evolution by DDSP in the presence of NHPI, pyridine, and 0.1 M ethylbenzene (EB) in CH_3CN under blue-light irradiation (λ = 467 ± 30 nm; 550 mW). The Ru(II) dye concentration was 100 μM for all reactions.

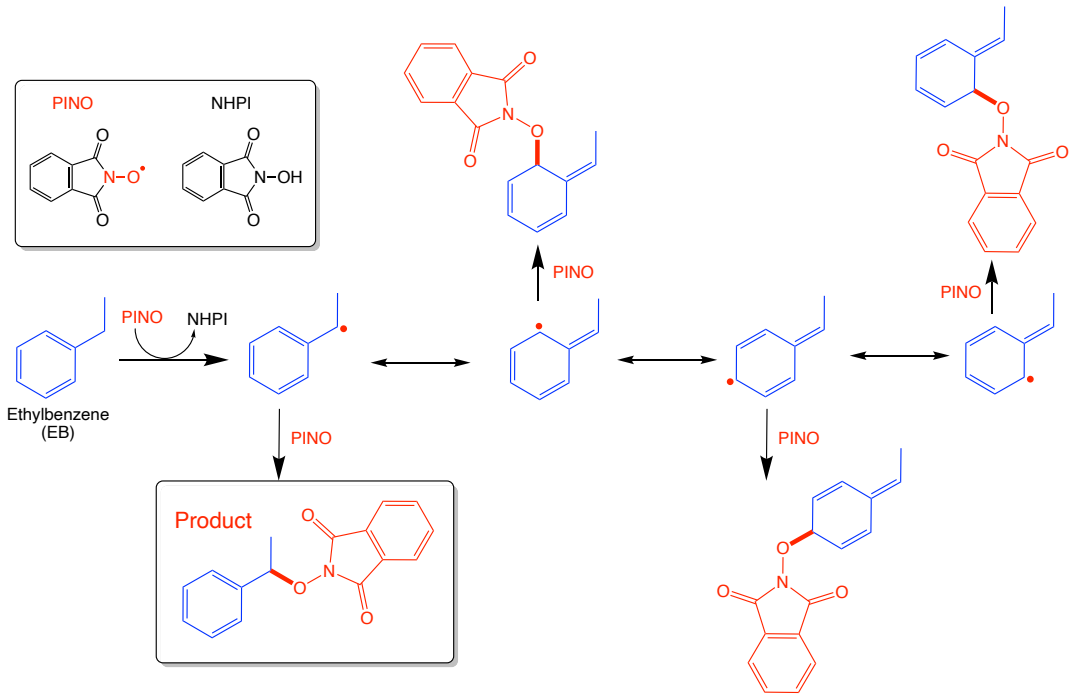

Scheme S1. Possible reaction mechanism to form several different byproducts.

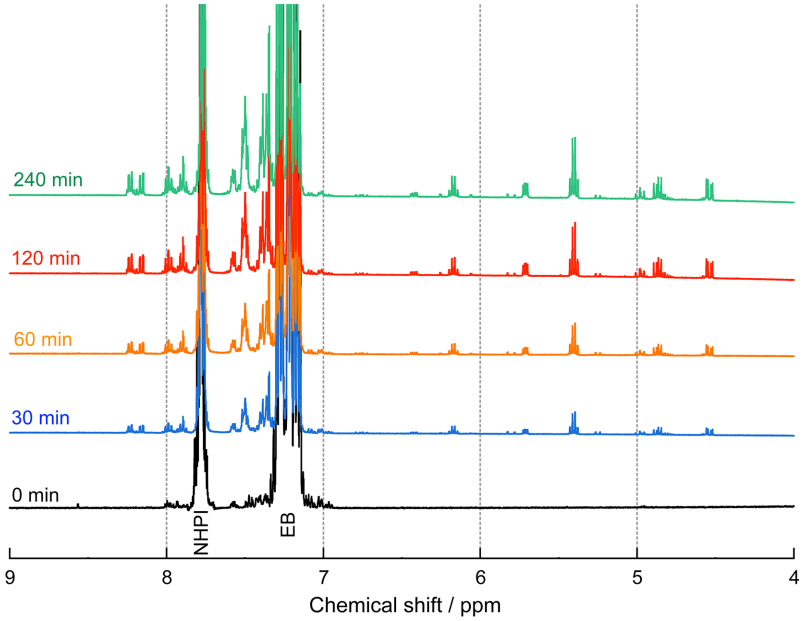

Figure S10. Changes of ^{1}H NMR spectrum of CH_3CN solution containing 30 mM NHPI, 50 mM pyridine-d^5, and 0.1 M ethylbenzene (black) before and after (blue) 30, (orange) 60, (red) 120, and (green) 240 min light irradiation with DDSP ([Ru] = 100 μM).

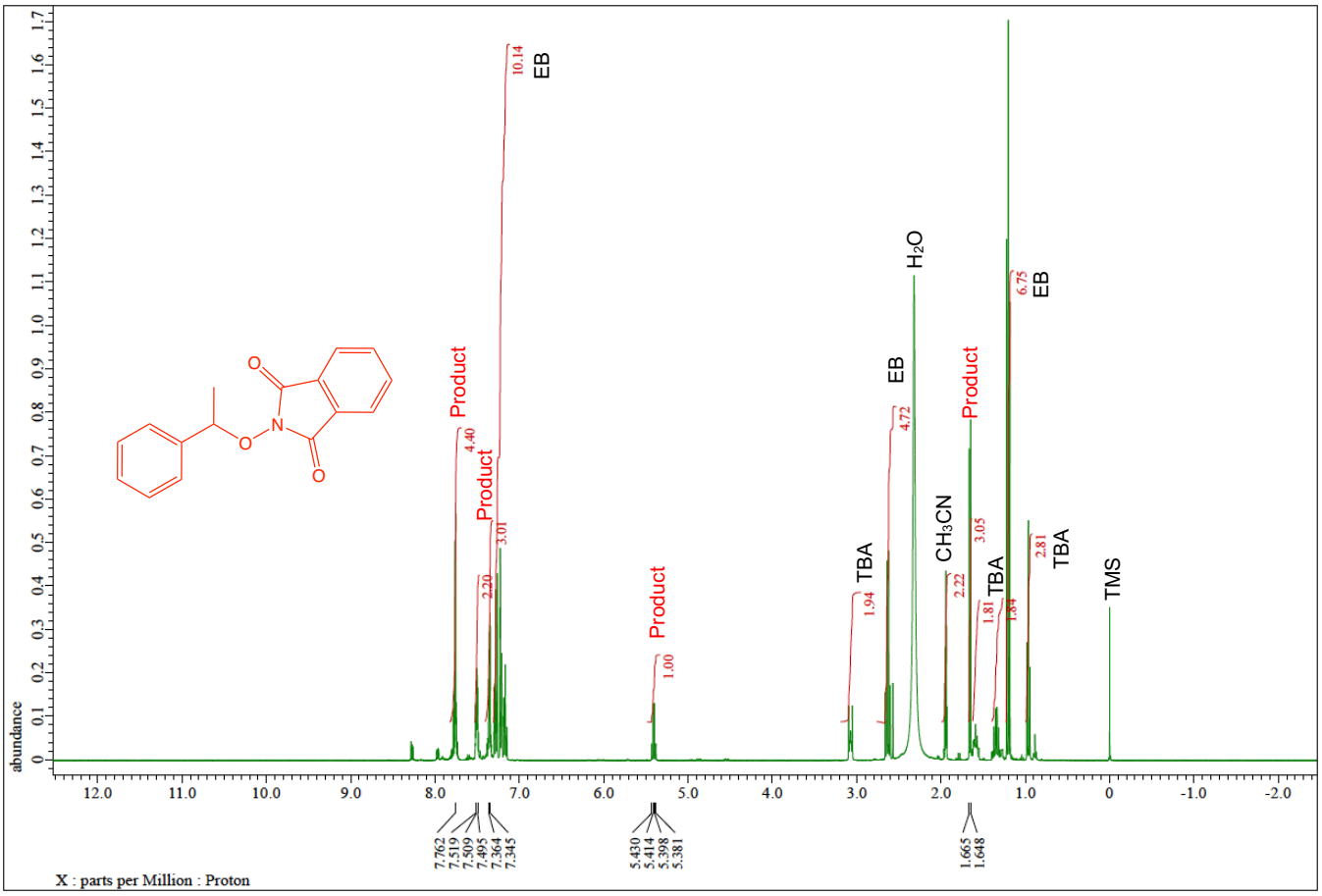

Figure S11. ^{1}H NMR spectra of the reaction supernatant obtained by 18 h photocatalytic H_2 production in the presence of DDSP ([Ru] = 100 μM), 30 mM NHPI, 50 mM pyridine-d^5, 5 mM tetrabutylammonium iodide (TBAI) and 0.1 M ethylbenzene (EB) in CD_3CN. The signals assigned to the radical coupling product (EB-PINO) between EB$^{\bullet}$ and PINO$^{\bullet}$ are labelled as "Product".

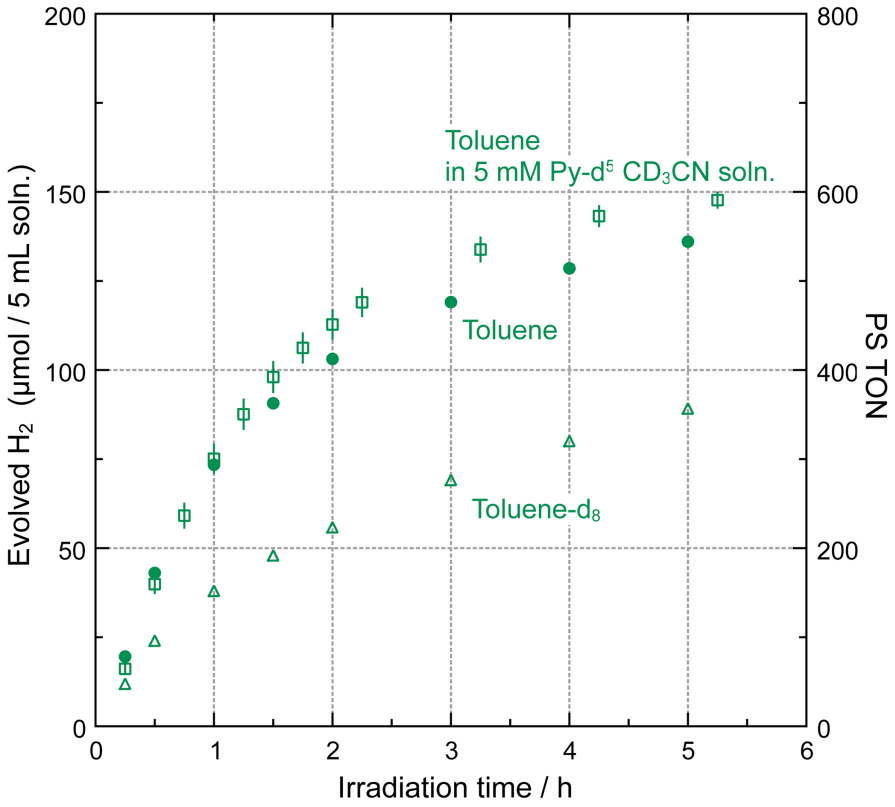

Figure S12. Photocatalytic H_2 evolution by DDSP in the presence of 30 mM NHPI, 50 mM pyridine and 0.1 M toluene (closed circles) or toluene-d^8 (open triangles) in CH_3CN under blue light irradiation (λ = 467 ± 30 nm; 550 mW). Open squares show the result in which pyridine and CH_3CN were replaced by their deuterated ones (Py-d^5 and CD_3CN). The Ru(II) dye concentration was 100 μM for all reactions.

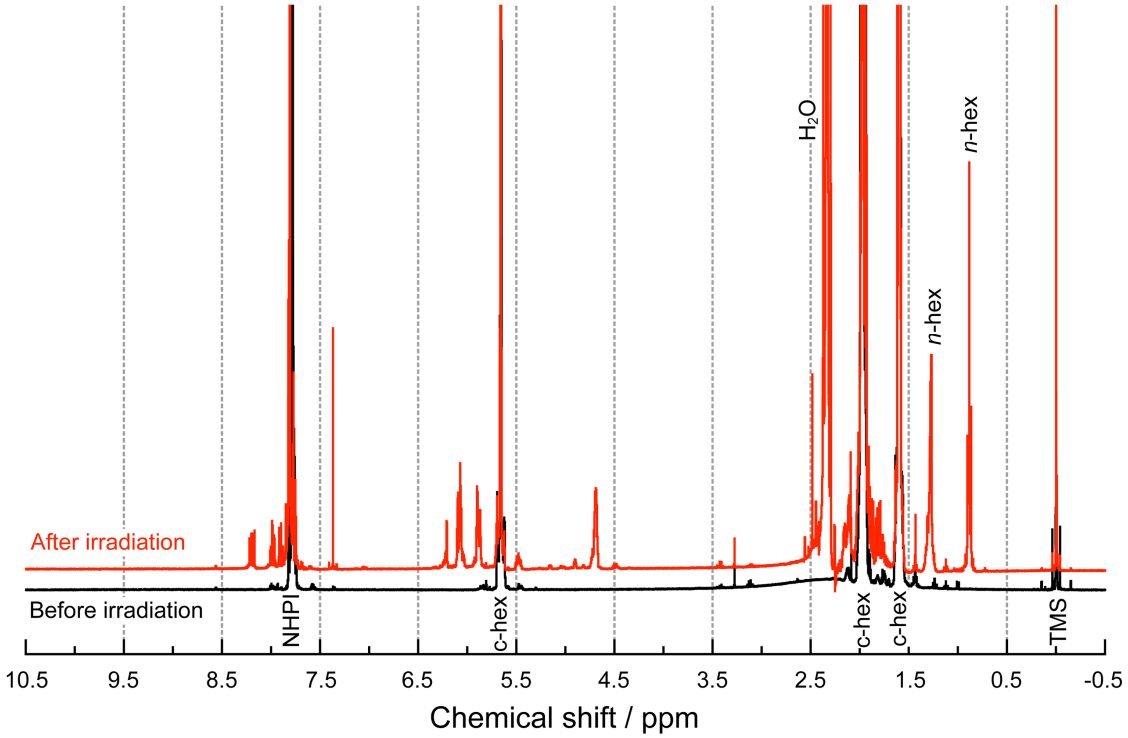

Figure S13. ^{1}H NMR spectra of CD_3CN solutions containing 30 mM NHPI, 50 mM pyridine-d^5, and 0.1 M cyclohexene (black) before and (red) after 5 h light irradiation with DDSP. Observed signals at 0.89 and 1.28 ppm labelled as "*n*-hex" are derived from slightly contaminated *n*-hexane used to remove vacuum grease.

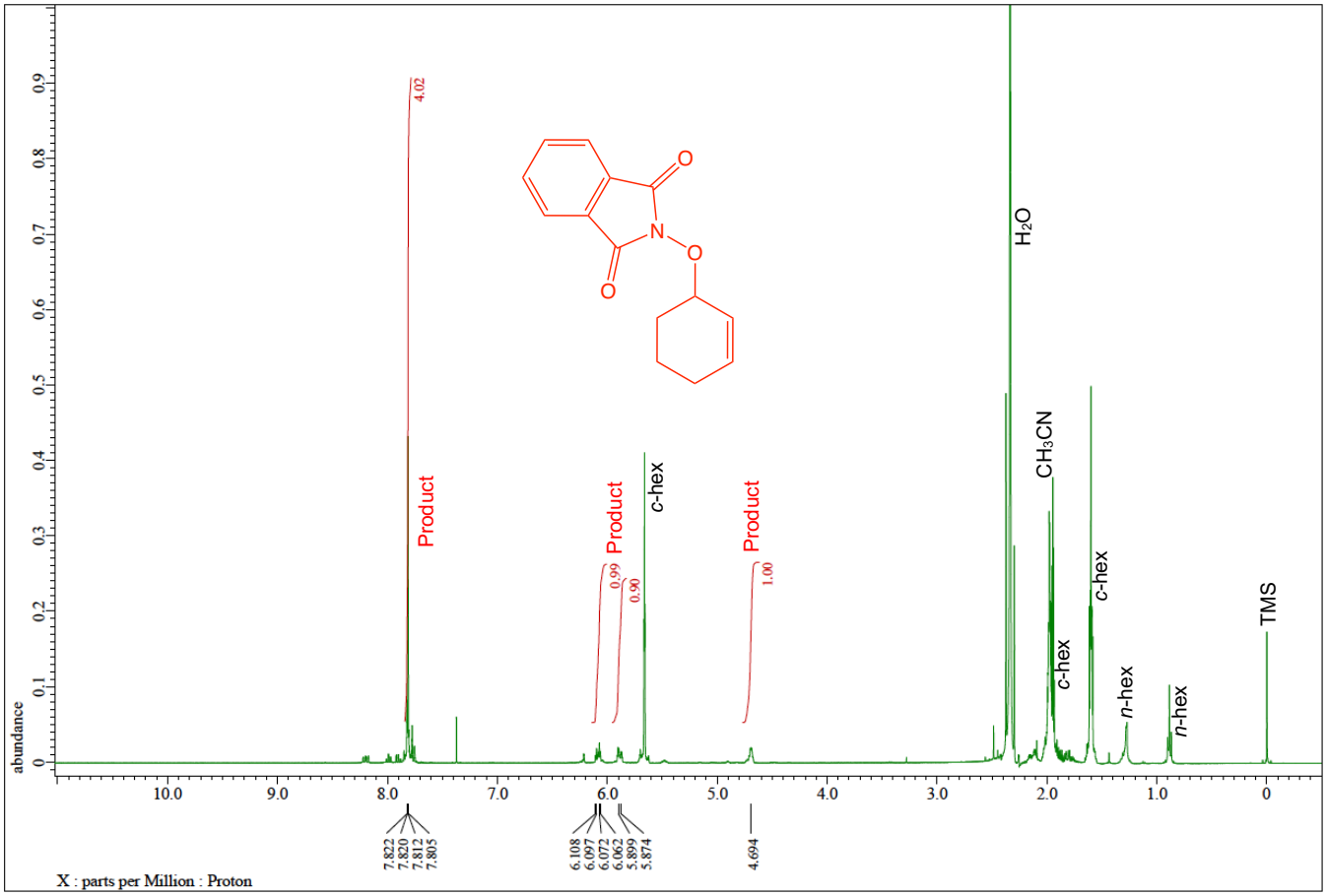

Figure S14. ^{1}H NMR spectra of the reaction supernatant obtained by 5 h photocatalytic H_2 production in the presence of DDSP ([Ru] = 100 μM), 30 mM NHPI, 50 mM pyridine-d^5, and 0.1 M cyclohexene in CD_3CN. The signals assigned to the radical coupling product (*c*-hex-PINO) between *c*-hex$^{\bullet}$ and PINO$^{\bullet}$ are labelled as "Product". Observed signals at 0.89 and 1.28 ppm labelled as "*n*-hex" are derived from slightly contaminated *n*-hexane used to remove vacuum grease. Signals of the aliphatic protons of *c*-hex-PINO at the cyclohexene ring would be overlapped with that of unreacted *c*-hex.

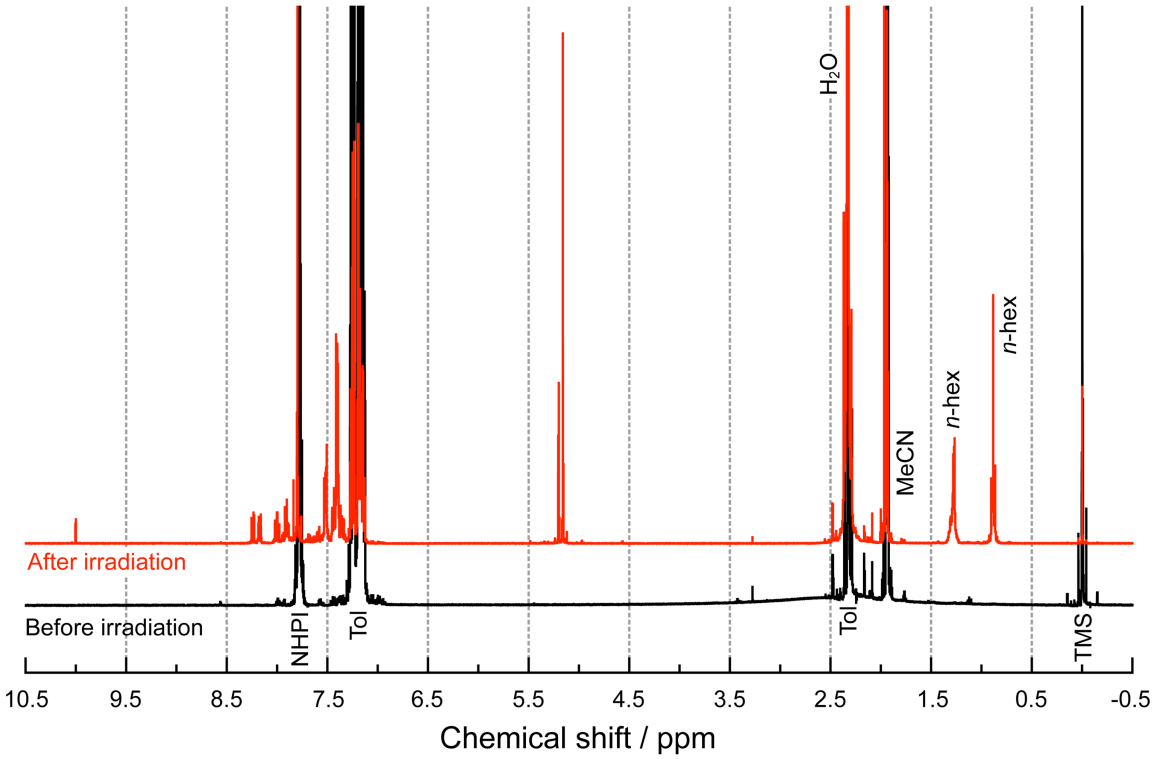

Figure S15. ^{1}H NMR spectra of CD_3CN solutions containing 30 mM NHPI, 50 mM pyridine-d^5, and 0.1 M toluene (black) before and (red) after 5 h light irradiation with DDSP. Observed signals at 0.89 and 1.28 ppm labelled as "*n*-hex" are derived from slightly contaminated *n*-hexane used to remove vacuum grease.

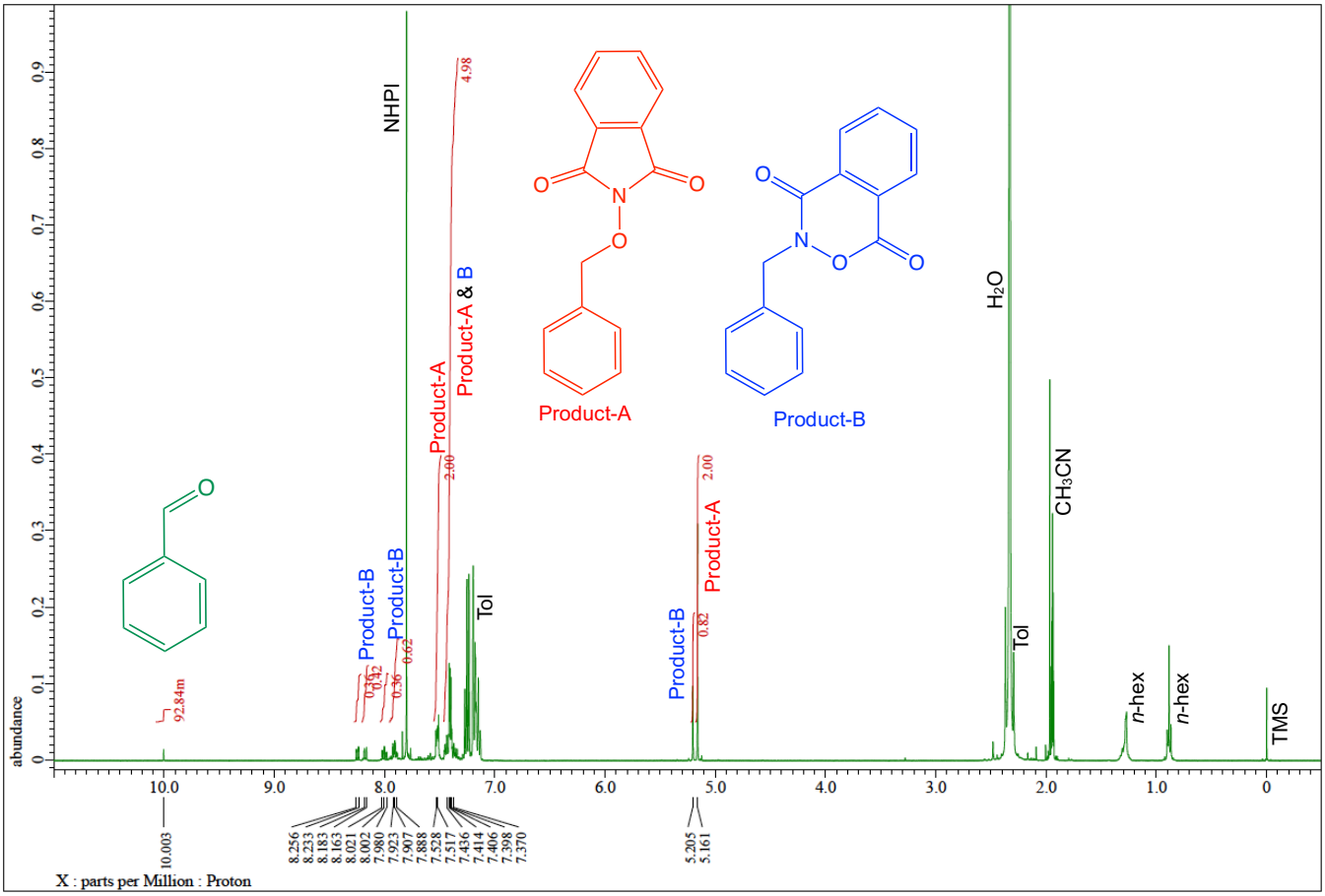

Figure S16. ^{1}H NMR spectra of the reaction supernatant obtained by 5 h photocatalytic H_2 production in the presence of **DDSP** ([Ru] = 100 μM), 30 mM NHPI, 50 mM pyridine-d^5, and 0.1 M toluene in CD_3CN. Signals assigned to the radical coupling products (Tol-PINO) between Tol$^\bullet$ and PINO$^\bullet$ are labelled as "Product-A" and "Product-B", according to the literature about the electrochemical Tol oxidation mediated by NHPI.[R4] Observed signals at 0.89 and 1.28 ppm labelled as "*n*-hex" are derived from slightly contaminated *n*-hexane used to remove vacuum grease.

References

R1. H. Park, W. Choi, M. R. Hoffmann, Effects of the preparation method of the ternary CdS/TiO_2/Pt hybrid photocatalysts on visible light-induced hydrogen production. *J. Mater. Chem*., 2008, **18**, 2379–2385.

R2. K. Hanson, M. K. Brennaman, A. Ito, H. Luo, W. Song, K. A. Parker, R. Ghosh, M. R. Norris, C. R. K. Glasson, J. J. Concepcion, R. Lopez, T. J. Meyer, Structure−Property Relationships in Phosphonate-Derivatized, Ru^{II} Polypyridyl Dyes on Metal Oxide Surfaces in an Aqueous Environment. *J. Phys. Chem. C*, 2012, **116**, 14837–14847.

R3. N. Yoshimura, A. Kobayashi, M. Yoshida, M. Kato, Enhancement of Photocatalytic Activity for Hydrogen Production by Surface Modification of Pt-TiO_2 Nanoparticles with a Double Layer of Photosensitizers, *Chem. Eur. J.*, 2020, **26**, 16939–16946.

R4. M. A. Hoque, J. Twilton, J. Zhu, M. D. Graaf, K. C. Harper, E. Tuca, G. A. DiLabio, S. S. Stahl, Electrochemical PINOylation of Methylarenes: Improving the Scope and Utility of Benzylic Oxidation through Mediated Electrolysis, *J. Am. Chem. Soc.*, 2022, **144**, 15295-15302.